Surface Integrity and the Influence of Tool Wear in High Speed Machining of Inconel 718

**Ru Lin Peng[1,*], Jinming Zhou[2], Sten Johansson[1], Annethe Billenius[1]
Volodymr Bushlya[2], Jan-Eric Stahl[2]**

[1] Department of Management and Engineering, Linköping University, 58183 Linköping, Sweden
[2] Department of Mechanical Engineering, Lund University, 22100 Lund, Sweden
* Corresponding author: ru.peng@liu.se

Abstract The influence of high speed turning and tool wear on the microstructure and residual stresses of Inconel 718 was investigated. The turning was performed using whisker reinforced alumina ceramic inserts and a cutting fluid. By electron channelling contrast imaging in SEM, significant microstructural changes, including grain-refinement in a thin surface layer and heavily deformed microstructure to a certain depth, were observed in turning using a new tool. X-ray diffraction measurements also revealed a characteristic residual stress field with surface tensile stresses and subsurface compressive stresses. With the development of wear in the tool flank, mechanical forces and heat involved in the cutting operation increased, leading to a much larger cutting affected zone and more drastic changes in the surface integrity. High surface tensile residual stresses, up to 1500 MPa, and dissolution of reinforcing precipitates and recrystallization of the surface layer were induced by severe tool wear, both of which can significantly affect the fatigue strength of the machined part.

Keywords High speed machining, Surface integrity, Residual stress, Tool wear, Inconel 718

1. Introduction

Various machining operations such as turning, milling and drilling are widely employed to create designed shapes and dimensions of engineering parts with the help of cutting tools. During such a manufacturing process, material is removed from the surface of a part with the help of a cutting tool, causing severe localized plastic deformation and shearing. Because of the mechanical work done and friction between the cutting tool and both the newly formed workpiece surface and the chip, the temperature in the cutting zone is unavoidably raised. The nature of such a process involving localized plastic deformation and heating means structural development and thereby property changes in the surface as well as subsurface of the machined part. Plastic deformation, heat induced microstructural changes, hardness variations and residual stresses are frequently observed in the cutting affected zone [1-4]. Such changes may have a direct impact on the performance and reliability of machined parts and therefore are constantly a subject of interest in research.

The current project investigates the influence of high speed turning on the surface integrity of nickel based superalloy Inconel 718. Nickel based superalloys have good strength as well as excellent oxidation and corrosion resistance at elevated temperatures. They constitute a very important group of structural materials suitable for high temperature applications in the aerospace and energy conversion industries. However, the alloys are also known as hard-to-cut materials due to their high strain hardening rate, poor heat conductivity and high-temperature strength. The poor machinability not only contributes to a low material removal rate but also induces rapid tool wear [5] which changes the cutting geometry of the tool. For wear in the tool flank, the increased tool-workpiece contact area and vanished clearance angle lead to increased mechanical forces and heat generation during cutting [5]. As a result, machining influence on the surface integrity of the workpiece is enhanced [4]. Microstructure alterations and residual stresses in turning of Inconel 718 by worn tools were studied in a few publications. Sharman et al. through optical microscopy and microhardness testing revealed that tool wear during turning of Inconel 718 increased the plastic

deformation depth, and at the higher speed end of the studied range of 40–120 m/min it also enhanced strain hardening of the subsurface [5]. Analysis by high resolution imaging of electron channeling contrast (ECC) in backscatter detectors and electron backscatter diffraction (EBSD) revealed that recrystallization and partial recrystallization also occurred in an immediate subsurface layer of 200–300 nm at a cutting speed of 300 m/min [6]. In [7], tool wear was reported to promote the formation of a so called white layer, independent of the application of coolant. Cutting using a worn tool is often found to increase the surface tensile residual stresses. In turning of Inconel 718 at low cutting speed (40 m/min), high surface tensile residual stresses up to 1043 MPa were reported in a surface prepared using a worn tool and the surface tensile stresses was found to decrease with increasing cutting speed [8]. For face finishing turning of RR1000 alloy, residual stress profile measurements revealed that tool flank wear not only increased the surface tensile residual stresses but also extended the compressive peak stresses to a larger depth [9].

This paper presents results from studies on the evolution of microstructural changes and residual stresses with the development of tool wear for high speed turning of Inconel 718 at 200 m/min with a cutting fluid. The influence of tool wear on residual stresses for cutting using the same tooling conditions but without the application of cutting fluid can be found in [10]. In [6], research work on subsurface deformation and their correlation to tool wear for turning at higher speed was reported.

2. Experimental Details

2.1. Material and machining operations

The Inconel 718 used in the current investigation has a nominal composition of: 53.8% Ni, 18.1% Cr, 5.5% Nb, 2.9% Mo, 1% Ti, 0.55% Al, 0.25% C, 0.04% Si and balance Fe (in weight). Round bars of 70 mm diameter and 200 mm length were received in solution annealed and aged condition with a nominal bulk hardness of 45±1 HRC. The backscatter electron images in Fig. 1 reveals a microstructure of equiaxed γ grains of nickel solid solution strengthened by very fine intermetallic γ" (coherent body centered tetragonal Ni_3Nb) particles visible at higher magnification. Elongated δ (an incoherent orthorhombic Ni_3Nb) particles are observed at grain-boundaries with some of them penetrating deep into the grains.

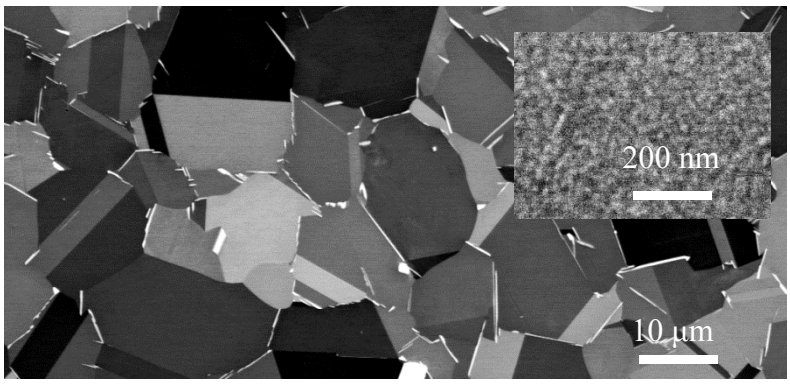

Fig. 1 Backscatter electron image of the as received alloy with a nickel base solid solution γ and reinforcing γ" precipitates (the inset). The elongated bright particles often located at grain boundaries are δ precipitates.

The as-received bars were machined down to 40 mm before further turning using whisker reinforced alumina ceramic (Al_2O_3+SiC_w) tools to prepare samples for the investigation. The cutting tool had a honed cutting edge and negative rake chamfer (0.1x20^o). The insert was mounted in a CDJNL3025P11 (ISO) type tool holder with a tool geometry of -6^o rake angle, 6^o clearance angle,

93^o edge major tool cutting and -6^o cutting edge inclination angle. To investigate the influence of tool wear on the machined surface quality, samples were also prepared with used tools of two degrees of flank wear, namely semi-worn tools (VB_{max} = 0.15 mm) and worn tools (VB_{max} = 0.3 mm). The cutting speed, feed rate, and cutting depth were 200 m/min, 0.2 mm/revolution, and 0.3 mm, respectively. All machining trials were conducted on a SMT500 CNC turning machine with a spindle speed up to 4000 rpm and a drive motor rated up 70kW. The cutting fluid was Sitala D 201-03 (Shell) containing 5% of semi-synthetic emulsion in solution and provided with 5 MPa at 40 l/min through an orifice 5 mm in diameter.

2.1. Surface integrity characterization

X-ray diffraction stress analysis is based on evaluating changes in the interplanar spacings of certain (hkl)-planes, namely the elastic strains, from which the residual stresses responsible for causing the changes are derived. Measurements in the current study were carried out in ψ-mode [11] on a Seifert X-ray diffractometer. With ψ being the angle of sample tilt around an axis passing through the goniometer center in the diffractometer plane, the commonly used $\sin^2\psi$-method [11] was employed to calculate residual stresses from the interplanar spacing measurements made in multiple ψ angles. To obtain a stress value, thirteen ψ-angles spreading in equal $\sin^2\psi$ interval between ($\psi = -50^o$) and ($\psi = 50^o$) were used. Diffraction peaks from the nickel γ-220 reflection were obtained using the Cr-K_α radiation and a pinhole collimator of 2 mm diameter. The peak positions and widths were determined by curve fitting with two pseudo-Voigt functions for $K_{\alpha1}$ and $K_{\alpha2}$, respectively. The X-ray diffraction elastic constant for nickel γ-(220) plane, needed for the stress calculation, is 4.65×10^{-6} MPa^{-1} [12]. To obtain depth profiles of residual stresses, stepwise electrolytic polishing was employed to expose the underlying material for diffraction measurements. The stress profiles presented in this paper are as measured results without any correction for possible stress relaxation due to the electrolytic polishing.

Small samples were cut from the machined bars. A surface encompassing both the cut and feed directions was then mechanically ground and polished following a procedure for preparing samples for electron backscatter diffraction (EBSD) analysis. The microstructural characterization was carried out in a Hitachi SU-70 FESEM scanning electron microscope. Annular solid state backscatter detectors from Hitachi were used to obtain images of electron channeling contrast (ECC) from the polished surface. The plastic deformation depth was also characterized by measuring the density of low angle grain boundary (LAGB) in EBSD using a Nordlys detector from Oxford Instruments. Scans with a step size of 0.5 μm were then performed along lines perpendicular to the cutting surface. The LAGB was defined as a misorientation of 1 to 10 degrees between two contiguous measurement positions along a scanned line. Its density at a particular sample depth was then calculated by averaging the number of lines containing a LAGB at the depth over the total number of scanned lines.

3. Results and Discussions

3.1 Microstructure of machining affected zone

As a reference state to illustrate the effect of dry cut, microstructure in the sample prepared using a new tool was briefly described in [10]. A more detailed analysis with regards to the cutting induced plastic deformation and temperature rise is given here. Fig. 2(a) presents an overview of microstructural alterations in the cutting affected zone. A plastic deformation gradient varying from surface towards depth is revealed by the ECC. Lattice distortions visible as contrast variations are seen at a depth up to about 60 μm. This zone, corresponding to the deformation depth indicated by

the LAGB density profile from EBSD line scans (Fig. 3(a)), is hereafter termed heavy deformation zone. Although slip bands related to cutting induced plastic deformation can be found in grains at a larger depth, the analysis here is limited to the zone of heavy deformation. Different microstructural features identified along the depth near the machined surface are shown in Fig. 2(b). In the outmost surface, Fig.2(c) discloses a discontinuous layer of less than 1 μm thick, distinguished from the material beneath by its very fine structure consisting of elongated grains lying in the cutting direction and some equiaxed grains. Such a layer with ultrafine or nano-sized grains has been reported in surfaces machined under certain cutting conditions [13,14] and is often attributed to severe plastic deformation with possible influence of a high temperature. In the current sample, deformation bands extended from the layer beneath are still recognizable and fragmented δ-particles are visible (Fig. 3(c)). These observations imply that severe plastic deformation is the main cause of the grain-refinement but the cutting heat may cause recovery and even partial recrystallization, producing the sharp boundary to the layer beneath.

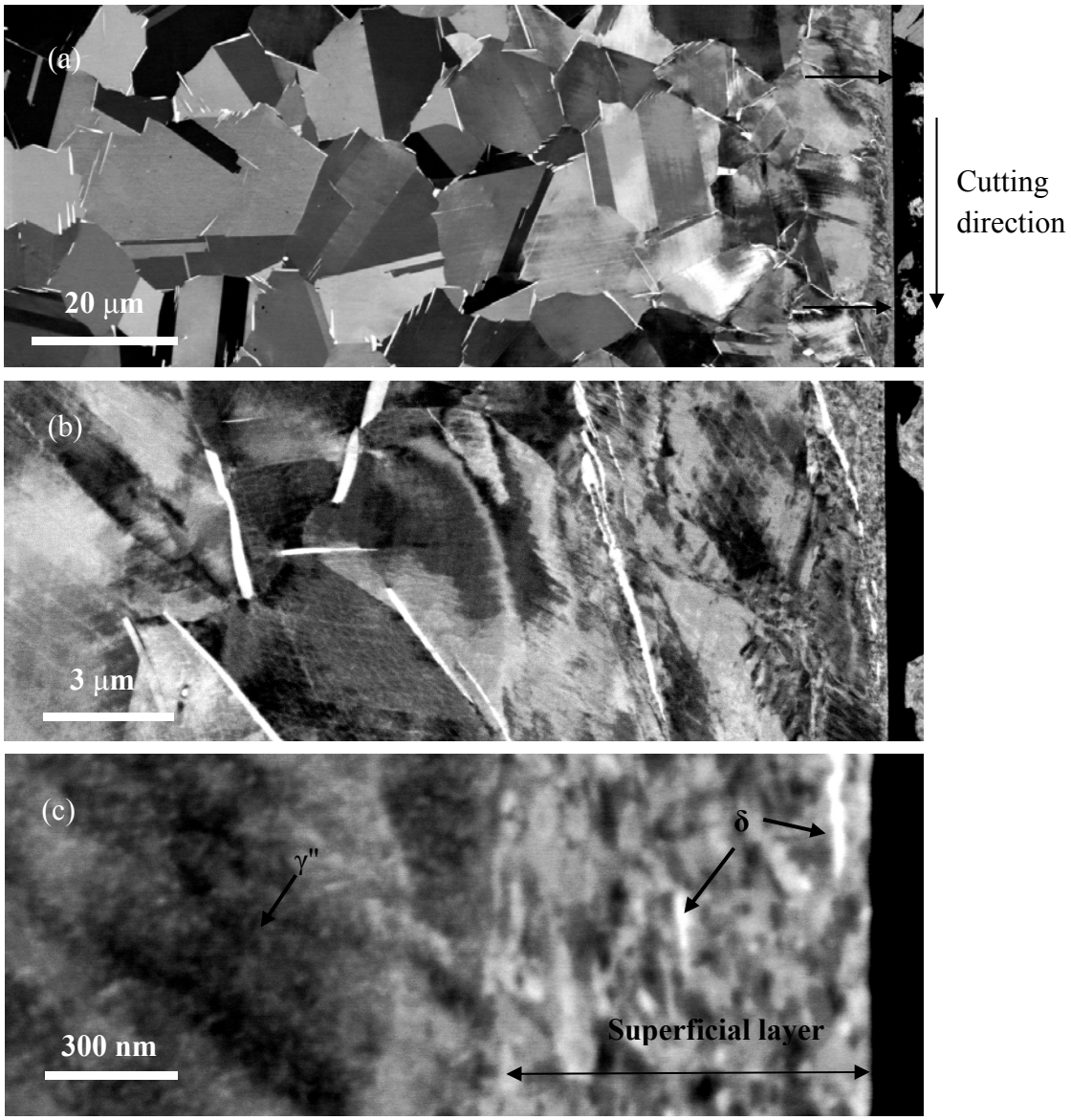

Fig. 2 Backscatter images showing microstructural alternations in machining affected zone of the sample prepared using a new tool. The machined surface is indicated by the arrows.

The next layer which extends to a depth of 10 to 25 μm contains severely deformed grains (Fig. 2(b)). In the literature, distorted grain boundaries and deformation bands are frequently reported from optical microscopic study on etched surfaces, see for example [7]. In comparison, the backscatter image in Fig. 2(b) reveals finer microstructural features such as fine slip bands and concentrated plastic strains in the vicinity of grain boundaries. As can be seen in the region close to the superficial layer, elongated grains inclining towards the cutting direction prevail. Stretching and rotation of the grains are accomplished by shear, leaving dense deformation bands extending over the grains. In many grains, the deformation bands tend to bend towards the cutting direction with rather abrupt change of the bands orientation. Fine slip bands are also observed in the regions between the deformation bands. In other grains which are less distorted, dislocation slip on multiple slip systems results in cell-like features. The δ-precipitates in this zone either deform following the grain boundaries and/or are sheared together with the deformation bands. It can be concluded from the above observations that heat from the cutting process has little effect on the already deformed structure; the forced cooling by cutting fluid and the poor thermal conductivity of the superalloy prevent a large amount of the cutting heat from penetrating into the depth. The retained strain hardening effect is expected to locally increase the hardness but at a cost of the ductility. Deeper in the sample, plastic deformation is less significant. The grains are characterized by cross-slip bands but the grain boundaries remain essentially undistorted (Fig. 2(a)).

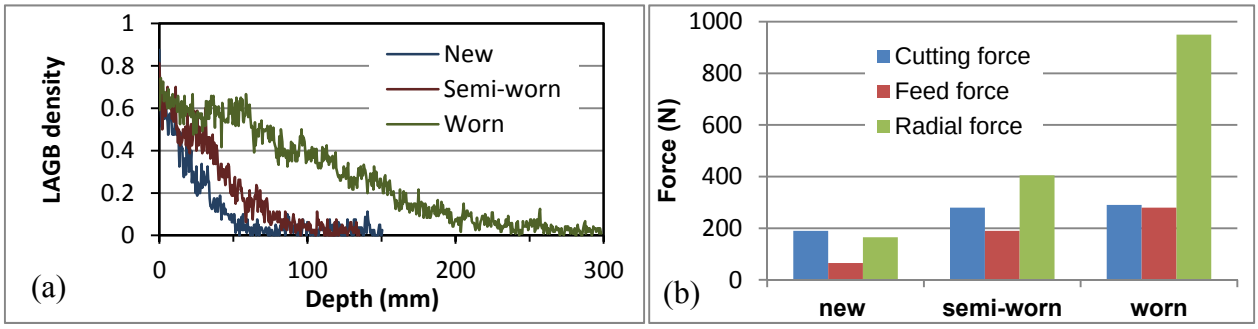

Fig. 3 Depth distribution of low angle grain boundary (a) and mechanical force components (b) for cutting under different tool conditions.

Cutting by a semi-worn tool with flank wear of VB_{max} = 0.15 mm leads to a larger cutting affected depth, as disclosed in Figs. 3(a) and 4(a). The depth of heavy plastic deformation shown in Fig. 4(a) is now slightly over 100 μm (Fig. 3(a)) and the severely deformed zone with distorted grains and grain boundaries extends to about 30 μm. The increased plastic deformation in association with tool wear is related to a higher cutting temperature and larger mechanical forces [5]. Wear in the tool flank results in a larger contact area between the tool and the sample surface as well as vanishing of the clearance angle. Subsequently, larger mechanical forces are required for material removal, as revealed by Fig. 3(b), leading to a larger deformation depth. Because of both the increased mechanical energy input and friction between the sample and tool, the cutting heat also increases which not only enhances plastic deformation by reducing the strength of the affected surface layer but also causes more significant microstructural changes. As can be seen in Fig 4(b), almost complete recrystallization occurs in the surface layer and partial recrystallization in some grain boundary regions beneath.

As a result of further increase in the mechanical forces (Fig. 3(b)) and heat, a much larger mechanical and temperature influence is found for cutting using a worn tool (VB_{max} = 0.3 mm). The heavy deformation depth reaches over 250 μm (Fig. 3(a)) with the severely deformed layer extending to about 60 μm below the surface (Fig. 5(a)). The fully recrystallized surface layer

containing equiaxed grains of over 100 nm in size and annealing twins becomes as thick as 3 μm (Figs. 5(b) and (c)). The strengthening γ'' particles completely disappeared from the layer, which may facilitate recrystallization of the layer. In some places, a very thin but extremely fine featured layer can be observed on top of the recrystallized zone, as can be seen in Fig. 5(c). This layer may form because of remelting by a high surface temperature [6] and quenching by the cutting fluid. Such changes in the microstructure greatly improves the surface ductility but at the cost of strength. In the depth between 2 to 10 μm, bands containing ultrafine, elongated or equiaxed grains or cell-structures associated with grain boundaries lie in a low angle to the cutting surface (Fig. 5(b)). It seems that as more cutting heat penetrates deeper into the material, the extremely distorted grain boundary regions may partly recrystallize. Between the heat affected grain boundaries are parallel short deformation bands and coarser cells formed by crossed slip bands. The rest of the heavy deformation zone shows similar microstructural feature to those in the samples prepared by the new tool and semi-worn tool.

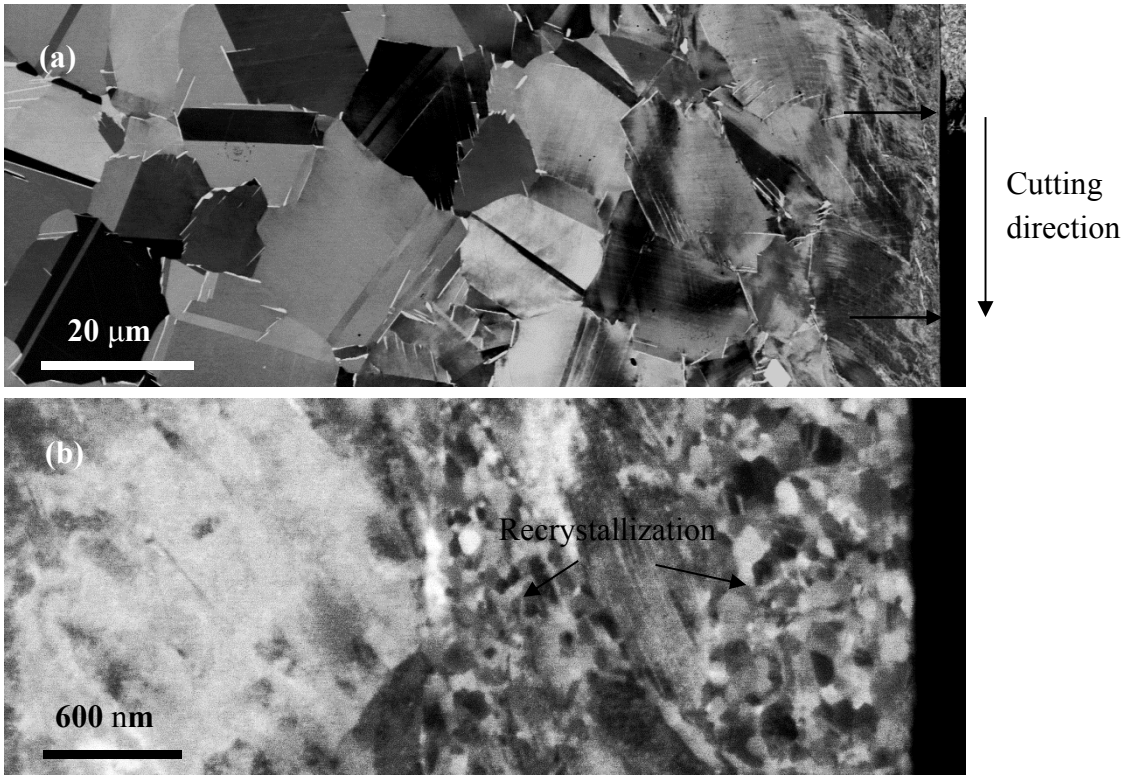

Fig. 4 Machining affected depth of the sample prepared by turning using a semi-worn tool.

3.2 Residual stresses

Residual stress profiles are presented in Fig. 6. As can be seen, tensile residual stresses are found in a thin surface layer and compressive stresses in the subsurface zone. The cutting tool condition affected both the extent of the tension and compression zones and the peak stress values. The diffraction peak width, given as full width at half maximum intensity (FWHM) in Fig. 6, is related to lattice distortion and grain size. Except for the surface layer containing ultrafine grains, the observed peak broadening can be attributed mainly to cutting induced plastic strains. The cutting affected depths indicated by the FWHM profiles are somewhat larger than that observed in Section 3.1 (Fig. 3(a)), indicating that X-ray diffraction is more sensitive for small plastic strains.

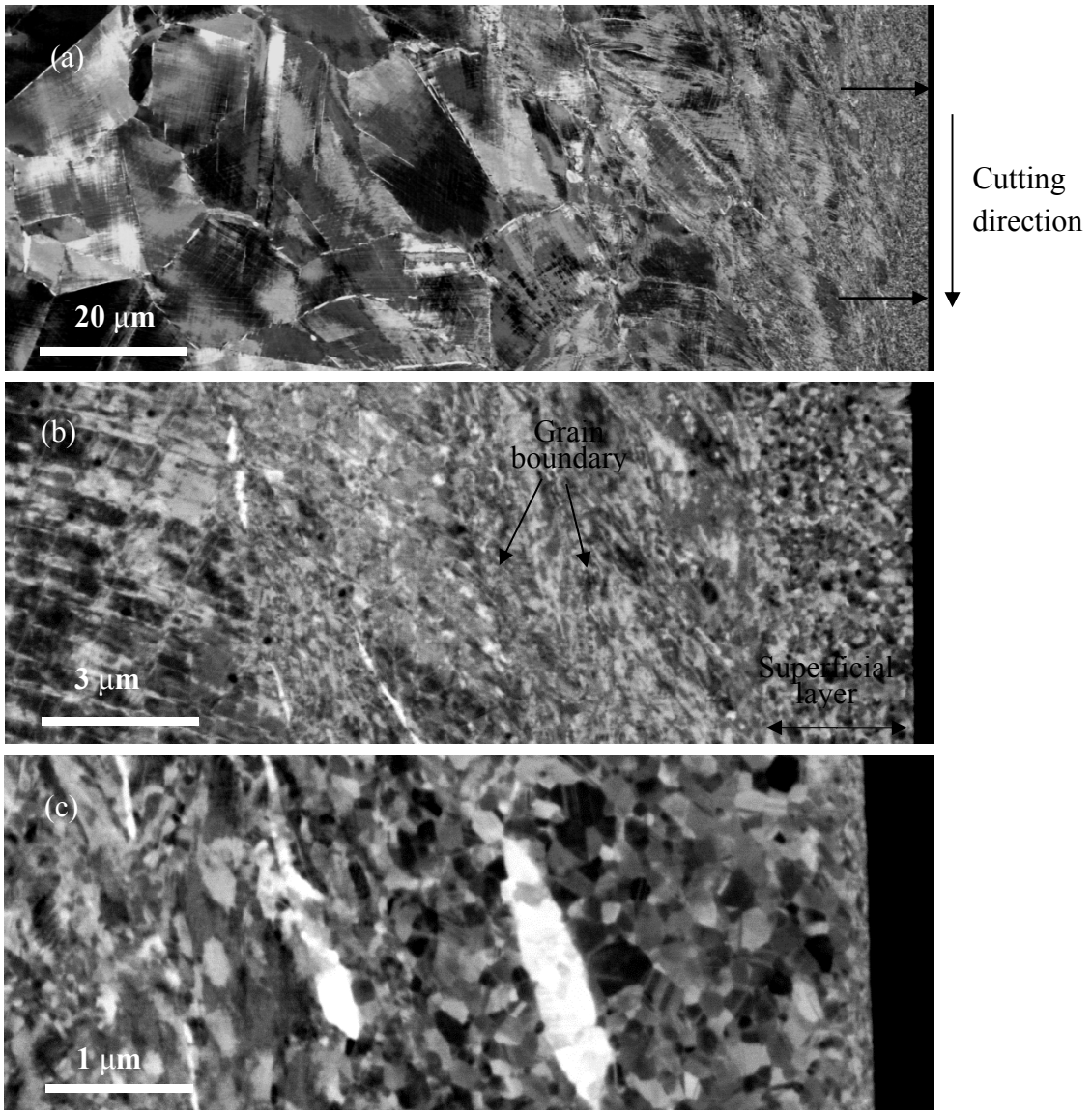

Fig. 5 Microstructure of the cutting affected depth prepared by a worn tool.

A 10 μm thick tensile zone with relatively low peak stresses is induced by cutting using the new tool, see Fig. 6(a). The residual stress field is slightly anisotropic, with a more rapidly decreasing stress in the feed direction. After reaching maximum compressive stresses at about 50 μm, both the stress components decrease, approaching zero at a depth of about 150 μm. The depth affected by plastic deformation reaches about 100 μm. A similar residual stress field with surface tensile stresses and subsurface compressive stresses has been reported for nickel-based alloys machined under different cutting conditions, for example, in the cutting speed range between 40 m/min and 120 m/min [8,15,16] and over 400 m/min [9,13,17]. Surface tensile stresses are often attributed to a dominant thermal effect from the cutting process [13,18]. When the contraction of a surface layer on cooling is hindered by the subsurface material of lower temperature, the surface layer will be put in tension and the subsurface layer in compression. On the other hand, plastic deformation involved in the cutting process which is mostly in-plane expansion has the opposite effect and will introduce compressive stresses in the surface layer [18]. Analogously, microstructural changes leading to a volume expansion of the surface layer will result in surface compression and subsurface tension. As analyzed in [10] for turning under the same cutting conditions but without the application of a cutting fluid, the observed stress field in Fig. 6(a) can be attributed to superposed mechanical and thermal effects: a somewhat anisotropic residual stress field with surface compression is induced by

surface plastic deformation and thermal stresses from cooling of a heated surface layer reverse the surface compression to tension.

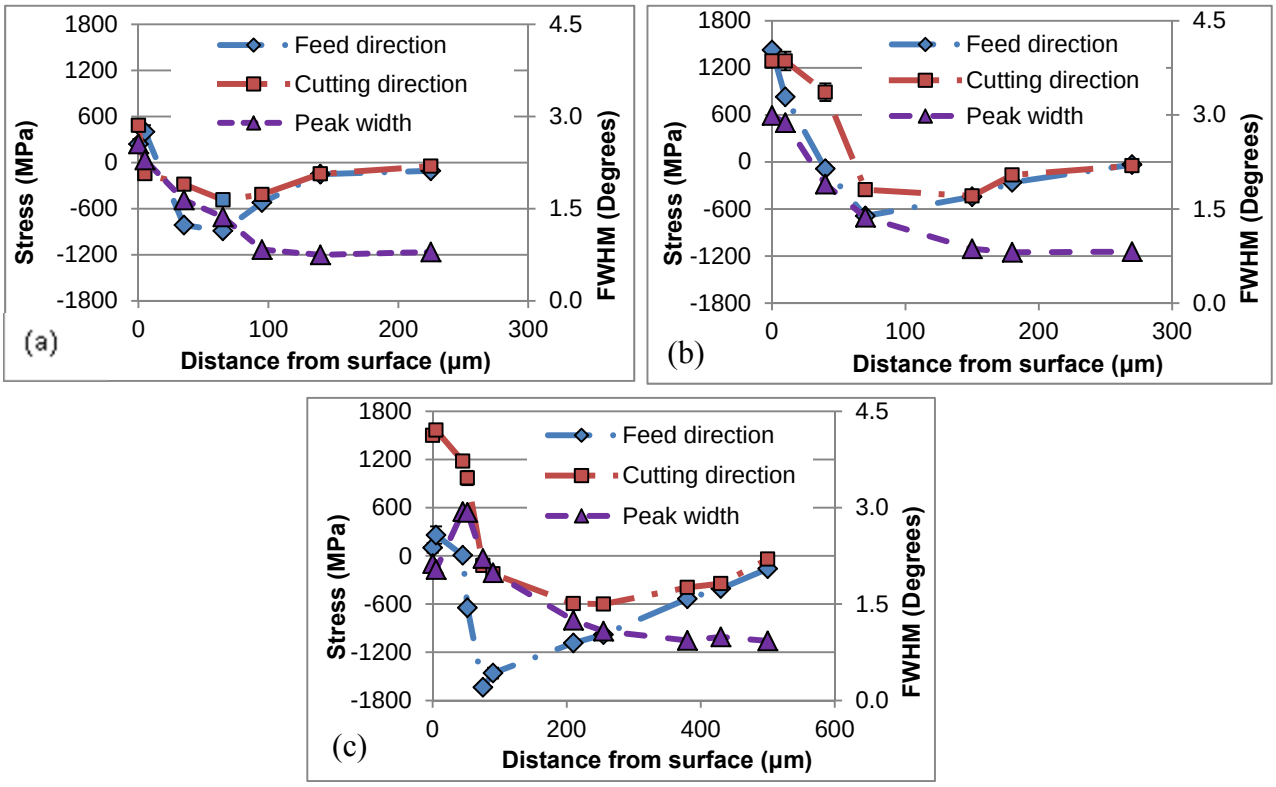

Fig. 6 Residual stresses and FWHM in the machining affected depth prepared using new tool (a), semi-worn tool (b) and worn-tool (c).

The higher cutting heat generated when using the semi-worn tool has a large influence on the surface tensile zone. The size of the zone is increased and the surface stresses are raised from about 240 MPa to 1400 MPa in the feed direction and 480 to 1300 MPa in the cutting direction (Fig. 6(b)). The higher mechanical forces (Fig. 3(b)) have little effect on the peak compressive stresses but enhance strain hardening in the near surface region, as revealed by the higher FWHM values, as well as expand the compression zone to a larger depth of 270 μm.

For the turning by the worn tool (VB_{max} = 0.3 mm), Fig. 6(c) reveals a surface tensile stress of 1500 MPa and a subsurface compressive peak of 600 MPa in the cutting direction. On the other hand, the surface tensile stress in the feed direction is reduced to 100 MPa, and at the same time the compressive stress peak is increased to about 1100 MPa. While the plastic deformation depth is further increased, to about 400 μm, recrystallization in the surface layer and partial recrystallization in the subsurface layer (Fig. 5) fully or partly removes the strain hardening effect, leading to low peak widths in the region (Fig. 6(c)). In spite of a stronger temperature effect on the microstructure, the observed residual stress anisotropy and the larger hardening depth suggest a more significant mechanical effect on the residual stress profiles in comparison with cutting using the semi-worn tool. The severe flank tool wear increases the feed and radial force components but has little effect on the cutting force component (Fig. 3(b)), which may result in a large difference between the two residual stress components. The recrystallization of the outer layer then relaxes the surface compressive stresses and residual stresses of tensile nature are generated later during cooling. It is interesting to compare the influence of tool wear with that of cutting speed for which increasing cutting speed also leads to a higher cutting temperature but lower mechanical forces [19] in contrast

to tool wear. Inspection of the results from face grooving of Inconel 718 published by Schlauer et al. [17] reveals that the increased thermal effect accompanying an increase in cutting speed from 410 m/min to 810 m/min enhances mainly surface tension and subsurface compression but has little influence on the stress anisotropy.

4. Conclusions

Electron channeling contrast imaging and X-ray diffraction were used to study machining induced microstructural changes and residual stresses, respectively, in Inconel 718 samples prepared by high speed turning under different cutting conditions. The following conclusions can be drawn from the investigation:

Mechanical forces and heat generated in the cutting process induced significant microstructural changes in the cutting affected zone. For cutting using a new tool, a surface layer of ultrafine grains formed because of local severe plastic deformation and high cutting heat. The layer beneath was heavily deformed, showing distorted grains and grain boundaries, deformation bands, and crossed slip bands; however, little influence of cutting temperature on the deformed microstructure was observed.

With the development of wear in the tool flank, the thicknesses of the fine-structured layer and the heavily deformed zone were increased as a result of increased mechanical forces and cutting heat. The temperature influence on the deformed microstructure was also enhanced. For turning using a worn tool, full recrystallization and dissolution of the strengthening γ" were observed in a surface layer up to several micrometer thick.

All the investigated samples showed a characteristic residual stress field with surface tensile stresses and subsurface compressive stresses, generated due to the localized plastic deformation and heating.

The increased cutting heat input and mechanical forces because of tool wear expanded both the tension and compression zones and resulted in much higher surface tensile stresses, up to 1500 MPa. When severe tool wear occurred, the residual stress field became strongly anisotropic, which could probably be ascribed to the different dependence of cutting force components on tool wear.

It has been shown that as tool wear progressed, surface damage in the form of microstructural alterations and tensile residual stresses increased. The level of tool wear is therefore crucial to the surface and subsurface quality of the machined part and severe tool wear may significantly affect its fatigue strength.

References

[1] R. M'Saoubi, J.C. Outeiro, H. Chandrasekaran, O.W. Dillon J., I.S. Jawahir, A review of surface integrity in machining and its impact on functional performance and life of machined products, International Journal of Sustainable Manufacturing. 1 (2008) 203-36.

[2] Y.B. Guo, W. Li, I.S. Jawahir, Surface integrity characterization and prediction in machining of hardened and difficult-to-machine alloys: a state-of-art research review and analysis, Mach. Sci. Technol. 13 (2009) 437-70.

[3] A. Devillez, G. Le Coz, S. Dominiak, D. Dudzinski, Dry machining of Inconel 718, workpiece surface integrity, J. Mater. Process. Technol. 211 (2011) 1590-1598.

[4] D. Ulutan, T. Ozel, Machining induced surface integrity in titanium and nickel alloys: A review, International Journal of Machine Tools & Manufacture. 51 (2011) 250-80.
[5] A.R.C. Sharman, J.I. Hughes, K. Ridgway, Workpiece surface integrity and tool life issues when turning Inconel 718 nickel based superalloy, Mach. Sci. Technol. 8 (2004) 399-414.
[6] J.M. Zhou, V. Bushlya, R.L. Peng, S. Johansson, P. Avdovic, J.-. Stahl, Effects of tool wear on subsurface deformation of nickelbased superalloy, Procedia Engineering 19 (2011) 407-413.
[7] V. Bushlya, J.M. Zhou, F. Lenrick, P. Avdovic, J. Stahlan, Characterization of white layer generated when turning aged inconel 718, 19 (2011) 60-66.
[8] A.R.C. Sharman, J.I. Hughes, K. Ridgway, An analysis of the residual stresses generated in Inconel 718 when turning, J. Mater. Process. Technol. 173 (2006) 359-67.
[9] W. Li, P.J. Withers, D. Axinte, M. Preuss, P. Andrews, Residual stresses in face finish turning of high strength nickel-based superalloy, J. Mater. Process. Technol. 209 (2009) 4896-902.
[10] R. Lin Peng, J.M. Zhou, J.M. S. Johansson, A. Billenius, V. Bushlya, J.-E. Stahl, Influence of dry cut and tool wear on residual stresses in high speed machining of nickel-based superalloy, To appear in Materials Science Forum. (2013).
[11] I.C. Noyan, J.B. Cohen, Residual Stress Measurement by Diffraction and Interpretation, (1987).
[12] P.S. Prevey, A method of determining the elastic properties of alloys in selected crystallographic directions for X-ray diffraction residual stress measurement, (1977) 345-54.
[13] C. Schlauer, M. Oden, Residual stress evolution and near-surface microstructure after turning of the nickel-based superalloy Inconel 718, Zeitschrift fur Metallkunde. 96 (2005) 385-92.
[14] R. Calistes, S. Swaminathan, T.G. Murthy, C. Huang, C. Saldana, M.R. Shankar, S. Chandrasekar, Controlling gradation of surface strains and nanostructuring by large-strain machining, Scr. Mater. 60 (2009) 17-20.
[15] J. Kenda, F. Pusavec, J. Kopac, Analysis of residual stresses in sustainable cryogenic machining of nickel based alloy - Inconel 718, J. Manuf. Sci. Eng. Trans. ASME. 133 (2011).
[16] D. Ulutan, M. Sima, T. Ozel, Prediction of machining induced surface integrity using elastic-viscoplastic simulations and temperature-dependent flow softening material models in titanium and nickel-based alloys, 223 (2011) 401-410.
[17] C. Schlauer, R.L. Peng, M. Oden, Residual stresses in a nickel-based superalloy introduced by turning, Mater. Sci. Forum. 404-407 (2002) 173-8.
[18] D.A. Axinte, R.C. Dewes, Surface integrity of hot work tool steel after high speed milling-experimental data and empirical models, J. Mater. Process. Technol. 127 (2002) 325-335.
[19] D. Dudzinski, A. Devillez, A. Moufki, D. Larrouquere, V. Zerrouki, J. Vigneau, A review of developments towards dry and high speed machining of Inconel 718 alloy, International Journal of Machine Tools & Manufacture. 44 (2004) 439-56.